Journal of Alloys and Compounds 501 (2010) 120–123

Contents lists available at ScienceDirect

Journal of Alloys and Compounds

journal homepage: www.elsevier.com/locate/jallcom

Surfactant-assisted solvothermal synthesis of single-crystalline ternary Bi–Sb–Te hexagonal nanoplates

Weili Ren*, Chunxia Cheng, Yongbin Xu, Zhongming Ren, Yunbo Zhong

Laboratory of Metallurgy and Materials Processing, College of Materials Science and Engineering, Shanghai University, Shanghai 200072, PR China

ARTICLE INFO

Article history:
Received 24 November 2009
Received in revised form 3 April 2010
Accepted 7 April 2010
Available online 18 April 2010

Keywords:
$(Bi,Sb)_2Te_3$
Nanoplates
Surfactant
Solvothermal

ABSTRACT

$Bi_{0.5}Sb_{1.5}Te_3$ hexagonal nanoplates have been successfully obtained by a simple solvothermal method assisted by the surfactant CTAB. The result shows that the obtained nanoplates are single crystal and the perpendicular direction to nanoplate is along *c*-axis of lattice structure. The product morphologies can be tuned by changing the added content of surfactant CTAB and water/ethanol volume ratio. The surfactant oriented growth mechanism for hexagonal nanoplates of ternary $(Bi,Sb)_2Te_3$ is proposed.

1. Introduction

Bi_2Te_3-based alloy is known as the best thermoelectric materials currently available for application near room temperature. Recently, significant thermoelectric properties improvement in the bulk materials has been achieved by creating nanograins and nonostructures in the grains by a combination of nanopowder preparation and sintering technique [1–8]. The nanoparticles are produced by many methods, such as hydro/solvothermal methods [3,4], spin melting [1], ball milling [2,5,8]. The sintering technique in the materials mainly involves the hot pressing [2–4] and spark plasma sintering [5,7,8]. The resultant properties of the bulk materials are related to the size and morphology of nanograins and nonostructures in the grains [9]. Therefore, the regulation of size and morphology for ternary Bi_2Te_3-based nanocrystal is of great importance for the development of higher efficiency devices of thermoelectric application. Moreover, compared with the large quantities reports about regulating the morphology of binary $A_2^{V}B_3^{VI}$ compounds, the study about the controlling growth of the ternary $(Bi,Sb)_2Te_3$ or $Bi_2(Te,Se)_3$ nanocrystals is limited.

Among current methods for the synthesis of nanostructure thermoelectric materials, the chemical routes have the advantages of low synthesis temperature, flexible controllability and fine grain sizes in comparison with those traditional metallurgical processes. The binary Bi_2Te_3 nanostructure with various morphologies such as nanoparticles [10–12], nanosheets [13], nanowires [14,15], hollow nanospheres [16], nanotubes [17] and nanoplates [18,19] has been prepared by solvo/hydrothermal method, wet chemical reactions. $Bi_2(Te,Se)_3$ nanoparticle [20], $Bi_2Te_{2.7}Se_{0.3}$ and $Bi_{0.5}Sb_{1.5}Te_3$ nanocrystals [21], Bi_2Te_2Se and $BiSbTe_3$ hexagonal nanoplatelets are also synthesized by the chemical ways [22]. In this work, the morphology of ternary $(Bi,Sb)_2Te_3$ nanocrystal is tried to regulate and control by the solvothermal route. Large scales of two-dimensional hexagonal $Bi_{0.5}Sb_{1.5}Te_3$ nanoplates are fabricated. The product morphologies are controlled by changing the added quantities of surfactant CTAB and water/ethanol volume ratio. Finally, the surfactant oriented growth mechanism for the hexagonally nanoplates of ternary $(Bi,Sb)_2Te_3$ is proposed.

2. Experimental details

All the regents were bought from commercial channels and used without further purification. The typical synthesis procedure is as follows: different quantities of hexadecyltrimethylammonium bromide (CTAB) were dissolved into a 40 mL mixture solution of water and ethanol volume ratio (1:1, 1:2, 1:4, 1:6), followed by the addition of $BiCl_3$ (0.5 mol/l), $SbCl_3$ (1.5 mol/l) and Te (3 mol/l) and NaOH (0.27 g) and $NaBH_4$ (8 mol/l). The resulting precursor suspension was stirred vigorously for 0.5 h and then sealed into a Teflon-lined autoclave of 50 mL capacity. The autoclave was heated and maintained at 210 °C for 8 h. The products were filtered off, washed several times with distilled water and absolute ethanol, and then finally dried in a vacuum at 60 °C for 4 h.

The phase structures of the nanocrystal were investigated by X-ray diffraction (XRD) with a Rigaku D/MAX-2550P diffractometer using Cu Kα radiation (λ = 0.154056 nm). The morphologies and nanostructure of the obtained products were characterized by the scanning electron microscopy (SEM), transmission electron microscope (TEM), high-resolution transmission electron microscope (HRTEM), selected area electron diffraction (SAED) and the composition analysis was performed at a SEM with an attached energy dispersed X-ray spectrometer (EDS).

* Corresponding author. Tel.: +86 21 56335470; fax: +86 21 56331102.
E-mail address: wlren@staff.shu.edu.cn (W. Ren).

0925-8388/$ – see front matter © 2010 Elsevier B.V. All rights reserved.
doi:10.1016/j.jallcom.2010.04.056

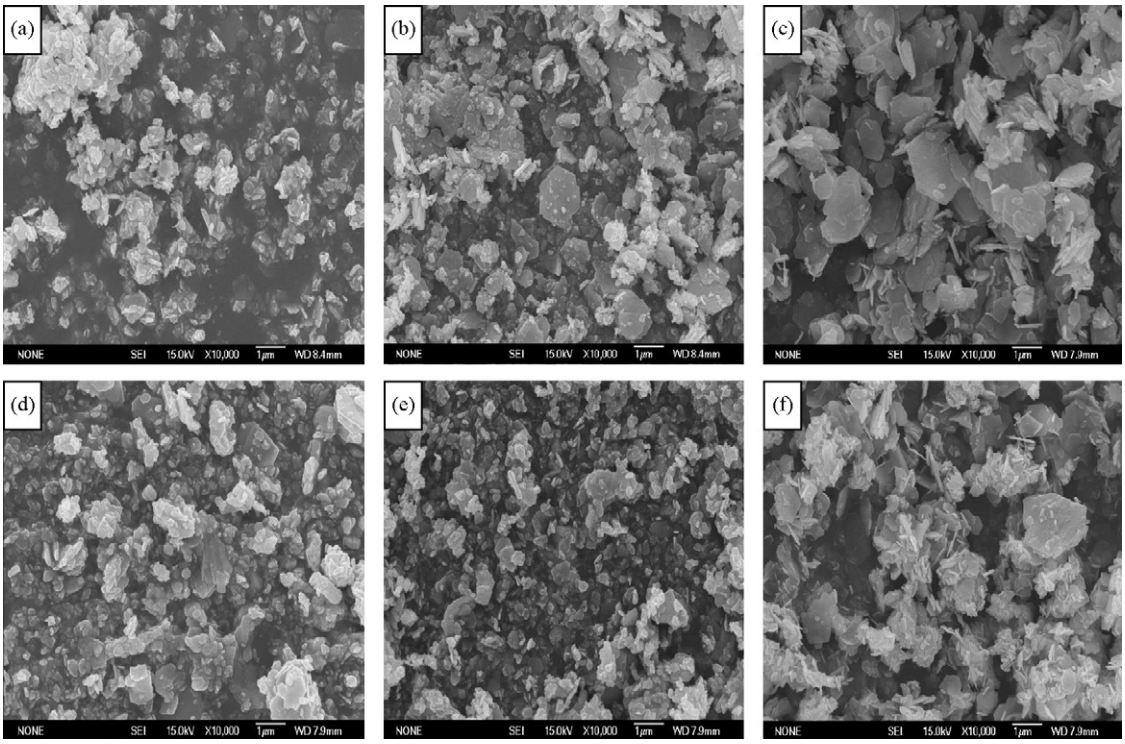

Fig. 1. The SEM images of the as-prepared ternary $(Bi,Sb)_2Te_3$ compounds in the various solvents and surfactant concentration. (a)–(c) Without CTAB, 0.1 g CTAB and 0.2 g CTAB, respectively, in the mix solvent of water and ethanol (volume ratio is 1:6); (d)–(f) the solvent volume ratio of 1:1, 1:2 and 1:4, respectively, with 0.2 g CTAB.

3. Results and discussion

Fig. 1 shows the morphologies of the as-prepared ternary $(Bi,Sb)_2Te_3$ compounds in the various solvents and surfactant concentration. It can be clearly seen that the morphologies of the obtained product are gradually from nanoparticles to hexagonally shaped nanoplates with the CTAB concentration and the ethanol volume ratio increasing.

The XRD pattern of $(Bi,Sb)_2Te_3$ nanocrystal synthesized in the water and ethanol volume ratio of 1:6 with 0.2 g CTAB (the same reaction condition as in Fig. 1c) is shown in Fig. 2b. All peaks in this pattern can be indexed according to JCPDS 49-1713 for $Bi_{0.5}Sb_{1.5}Te_3$. No remarkable diffractions of other phases such as Te, Bi or their compounds can be found, indicating that a pure

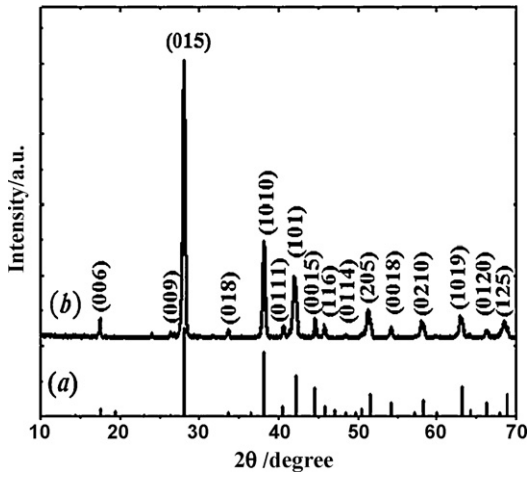

Fig. 2. (a) The pattern of JCPDS 49-1713; (b) the XRD pattern of the $Bi_{0.5}Sb_{1.5}Te_3$ nanocrystal synthesized in the water and ethanol volume ratio of 1:6 with 0.2 g CTAB.

$Bi_{0.5}Sb_{1.5}Te_3$ phase has been obtained under the current synthetic conditions. Due to the steric effect arising from the long alkyl chain of CTAB and the low surface tension and dielectric constant of the ethanol, the chemical reaction rate can be reduced with the CTAB concentration and ethanol volume ratio increasing. So it can be considered that the pure ternary $(Bi,Sb)_2Te_3$ nanocrystal can be obtained under all the condition given above in Fig. 1.

Fig. 3 shows the high magnification SEM image and TEM images of the as-prepared products in the water and ethanol volume ratio of 1:6 with 0.2 g CTAB. Fig. 3a–c reveals that typical products consist of large quantities of plate-like structures with about 100–450 nm in edge length and 30–90 nm in thickness. The SAED pattern shown in Fig. 3b′ exhibits a hexagonal symmetry diffraction spot pattern, which indicates its single crystal nature. The chemical composition of the nanoplates is further determined by energy-dispersive X-ray spectroscopy (EDS). The approximate element proportion of Bi, Sb and Te is 9.89:29.03:61.08 (at.%), which is in agreement with the nominal composition. The crystallinity and the growth direction of an individual nanoplate are analyzed by HRTEM. Fig. 3d–f is the HRTEM images of the marked area in Fig. 3c, which shows the nanoplates are high crystallized and free from dislocation and stacking faults. The lattice plane spacing is 0.2134 nm corresponding to the (1 1 0) planes of $Bi_{0.5}Sb_{1.5}Te_3$ as in Fig. 3f, which indicates the perpendicular direction to nanoplate is along *c*-axis of lattice structure.

The ternary $(Bi,Sb)_2Te_3$ nanocrystal is synthesized by the following chemical reaction:

$$Bi^{3+}(Sb^{3+}) + BH_4^- + OH^- \rightarrow Bi(Sb) + H_2BO_3^- + H_2 \quad (1)$$

$$Te + BH_4^- \rightarrow Te^{2-} + H_2BO_3^- + H_2 \quad (2)$$

$$Bi^{3+} + Sb^{3+} + Te^{2-} \rightarrow Bi_{0.5}Sb_{1.5}Te_3 \quad (3)$$

$$Bi + Sb + Te \rightarrow Bi_{0.5}Sb_{1.5}Te_3 \quad (4)$$

The above results show that the regular hexagonal nanoplate is gradually obtained with the surfactant CTAB concentration

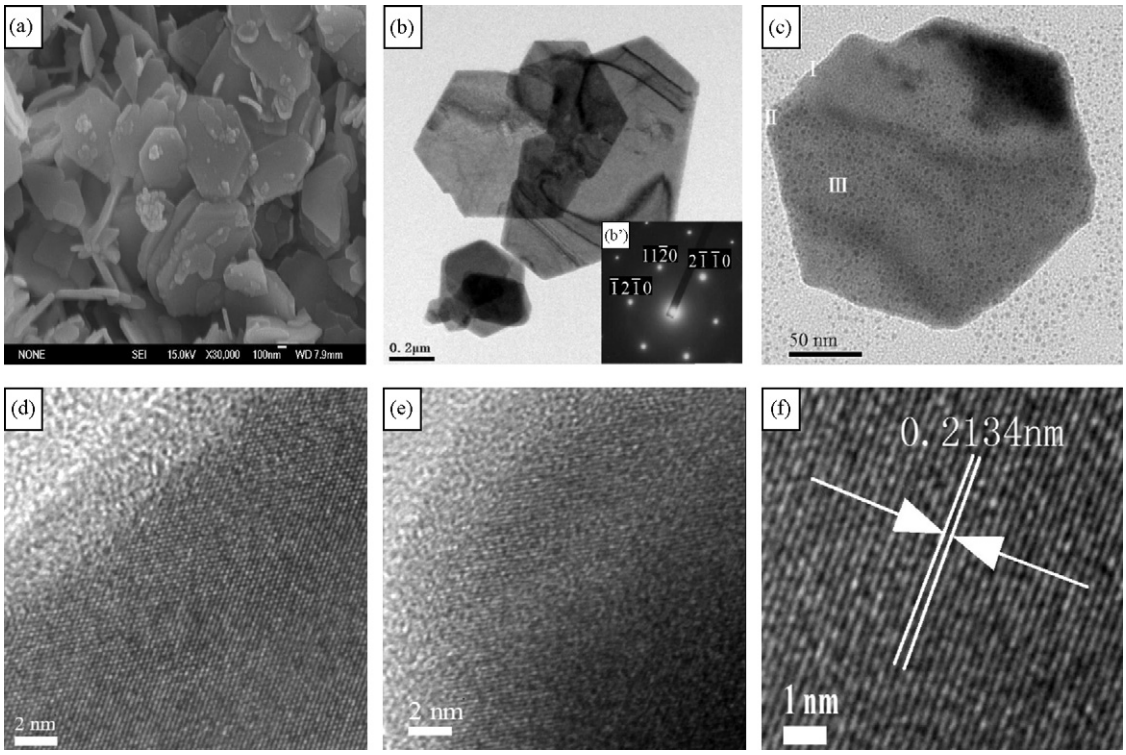

Fig. 3. The high magnification SEM and TEM images of $Bi_{0.5}Sb_{1.5}Te_3$ nanoplates synthesized in the water and ethanol volume ratio of 1:6 with 0.2 g CTAB: (a) high magnification SEM image; (b) and (c) typical TEM images of $Bi_{0.5}Sb_{1.5}Te_3$ nanoplates; (b′) SAED pattern of $Bi_{0.5}Sb_{1.5}Te_3$ nanoplates; (d), (e) and (f) HRTEM image of the marked area shown in (c).

and ethanol volume ratio increasing. $Bi_{0.5}Sb_{1.5}Te_3$ possesses a special anisotropic layer crystal structure arranged in the order of $Te^{(1)}$–Bi(Sb)–$Te^{(2)}$–Bi(Sb)–$Te^{(1)}$ along the *c*-axis direction. Two adjacent Te layers are bonded in van der Waals force, while others are covalent bonds. CTAB is a kind of cationic surfactant, which tends to selectively adsorb to a certain crystal plane of this intrinsic anisotropic crystal compounds during the growth. The selective adsorption of surfactants has also been reported in the references [15,18,19]. Therefore, it is reasonably deduced that CTAB oriented growth plays an important role in the morphology of $Bi_{0.5}Sb_{1.5}Te_3$ plate-like nanocrystals. The possible formation procedure for the hexagonally shaped $Bi_{0.5}Sb_{1.5}Te_3$ nanoplates mainly includes two steps: (i) the formation of small nascent crystal nuclei; (ii) the preferential growth of a certain crystal plane to form faceted (hexagonal) nanoplates with the help of selective absorption of CTAB molecules under the suitable condition. The sketch map of CTAB oriented growth is shown in Fig. 4. When the crystal nuclei are formed, the hydrophobic sides of CTAB are likely to selectively adsorb to a certain (1 1 0) crystal plane, which are supported by the pattern of selected area electron diffraction (Fig. 3b′). This blocks the growth along the *c*-axis and the ions and atoms of reaction source assemble in the layer edges of the crystal nuclei. The proposed procedure can be confirmed by the visual morphologies of time-dependent products for $Bi_{0.5}Sb_{1.5}Te_3$ nanostructures. Fig. 5 shows the SEM images of $Bi_{0.5}Sb_{1.5}Te_3$ nanoplates synthesized in the water and ethanol volume ratio of 1:6 with 0.2 g CTAB at different reaction time. A large amount of fine nanoparticles formed when the solvothermal reaction was processed for 1 h (Fig. 5a), which is accordance with the characteristics of the initial nucleation. When the reaction lasted for 2 h, some distinct plate-like shapes began to appear in the products (Fig. 5b). Increasing the reaction time to 8 h, almost all the products show the characteristics of hexagonal nanoplates, as shown in Fig. 1c.

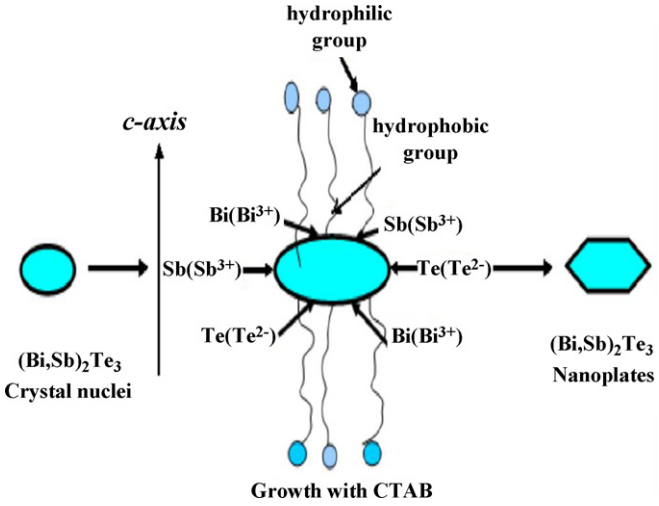

Fig. 4. The sketch map of the $(Bi,Sb)_2Te_3$ oriented growth with the surfactant CTAB.

The above-proposed mechanism is further supported by the effect of solvent volume ratio and CTAB concentration on the product morphologies in this study. As we know, the ethanol solvent can dramatically decrease the formation velocity of products owing to it low surface tension and dielectric constant as shown in Table 1 [23]. The steric effect of surfactant also decreases the reaction velocity.

Table 1
The physical properties of water and ethanol at 25 °C.

Solvent	Surface tension (10^{-3} N/m)	Dielectric constant
Water	71.81	78.3
Ethanol	22.1	24.5

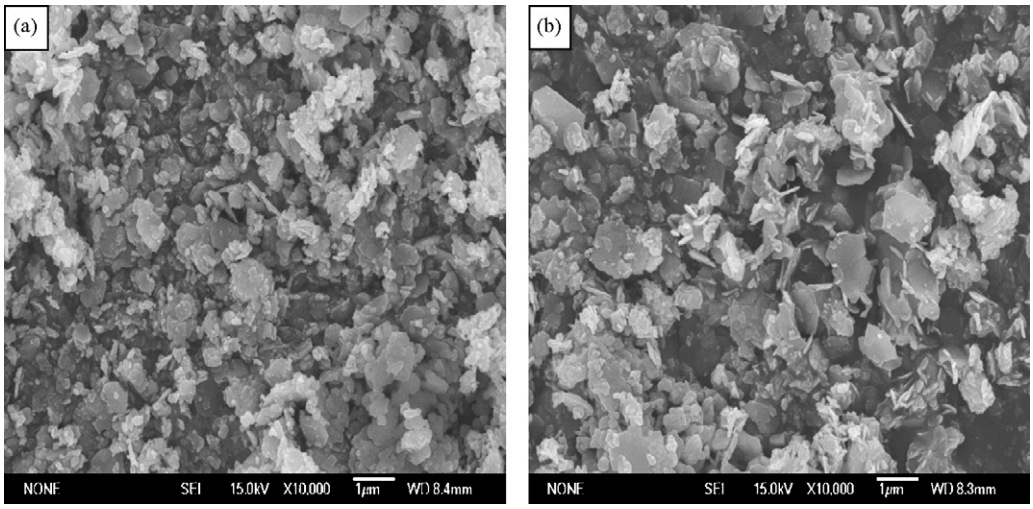

Fig. 5. The SEM images of $Bi_{0.5}Sb_{1.5}Te_3$ nanoplates synthesized in the water and ethanol volume ratio of 1:6 with 0.2 g CTAB at different reaction time: (a) 1 h; (b) 2 h.

When the ethanol volume rate is relatively low, a large quantity of crystal nuclei quickly form, which almost consumes all the reaction sources. CTAB oriented growth mechanism cannot play a role in the subsequent development of crystal nuclei. So when the water and volume ratio is 1:1 or 1:2, no plate-like structures can be found. The nanoplates only appear in the solvent volume ratio of 1:4 or 1:6. Since the added CTAB dramatically decreases the reaction velocity and provides the more oriented molecule for crystal nuclei, the ratio of nanoplate in the products gradually increases with the CTAB concentration increasing.

Therefore, the surfactant CTAB oriented growth should be responsible for the obtained nanoplate morphology of ternary $Bi_{0.5}Sb_{1.5}Te_3$ compound.

4. Conclusions

In summary, $Bi_{0.5}Sb_{1.5}Te_3$ single-crystalline nanoplates have been synthesized in large scale via a simple solvothermal method assisted by surfactant CTAB. The size of nanoplates is 100–450 nm in edge length and 30–90 nm in thickness. TEM and SAED patterns show that the as-prepared nanoplate is highly crystallized and free from dislocation and stacking faults. The product morphologies can be controlled by changing the added content of CTAB and water/ethanol volume ratio. The surfactant oriented growth mechanism for $Bi_{0.5}Sb_{1.5}Te_3$ nanoplates formation is proposed.

Acknowledgements

This work was supported by the National Natural Science Youth Foundation of China (No. 50701031) and by Program for Changjiang Scholars and Innovative Research Team in University (No. IRT0739).

References

[1] W.J. Xie, X.F. Tang, Y.G. Yan, Q.J. Zhang, T.M. Tritt, Appl. Phys. Lett. 94 (2009) 102111.
[2] B. Poudel, Q. Yao, Y. Ma, Y.C. Lan, A. Minnich, B. Yu, X. Yan, D.Z. Wang, A. Muto, D. Vashaee, X.Y. Chen, J.M. Liu, M.S. Dresselhaus, G. Chen, Z.F. Ren, Science 320 (2008) 634–638.
[3] X.B. Zhao, S.H. Yang, Y.Q. Cao, J.L. Mi, Q. Zhang, T.J. Zhu, J. Electron. Mater. 38 (2009) 1017–1024.
[4] Y.L. Li, J. Jiang, G.J. Xu, W. Li, L.M. Zhou, Y. Li, P. Cui, J. Alloys Compd. 480 (2009) 954–957.
[5] L.D. Zhao, B.P. Zhang, W.S. Liu, H.L. Zhang, J.F. Li, J. Alloys Compd. 467 (2009) 91–95.
[6] C.N. Liao, L.C. Wu, J.S. Lee, J. Alloys Compd. 490 (2010) 468–471.
[7] C.H. Kuo, C.S. Hwang, M.S. Jeng, W.S. Su, Y.W. Chou, J.R. Ku, J. Alloys Compd. 496 (2010) 687–690.
[8] L.D. Zhao, B.P. Zhang, J.F. Li, M. Zhou, W.S. Liu, J. Liu, J. Alloys Compd. 455 (2008) 259–264.
[9] A.J. Minnich, M.S. Dresselhaus, Z.M. Ren, G. Chen, Energy Environ. Sci. 2 (2009) 466–479.
[10] M. Salavati-Niasari, M. Bazarganipour, F. Davar, J. Alloys Compd. 489 (2010) 530–534.
[11] Y. Jiang, Y.J. Zhu, J. Cryst. Growth 306 (2007) 351–355.
[12] Y.Q. Cao, X.B. Zhao, T.J. Zhu, X.B. Zhang, J.P. Tu, Appl. Phys. Lett. 92 (2008) 143106.
[13] Q. Yao, Y.J. Zhu, L.D. Chen, Z.L. Sun, X.H. Chen, J. Alloys Compd. 481 (2009) 91–95.
[14] H. Yu, P.C. Gibbs, W.E. Buhro, J. Mater. Chem. 14 (2004) 595–602.
[15] T. Sun, X.B. Zhao, T.J. Zhu, J.P. Tu, Mater. Lett. 60 (2006) 2534–2537.
[16] Y. Jiang, Y.J. Zhu, L.D. Chen, Chem. Lett. 36 (2007) 382–383.
[17] Y.Q. Cao, T.J. Zhu, X.B. Zhao, J. Alloys Compd. 449 (2008) 109–112.
[18] Y.B. Xu, Z.M. Ren, W.L. Ren, G.H. Cao, K. Deng, Y.B. Zhong, Mater. Lett. 62 (2008) 4273–4276.
[19] Y.B. Xu, Z.M. Ren, G.H. Cao, W.L. Ren, K. Deng, Y.B. Zhong, Mater. Lett. 62 (2008) 4525–4528.
[20] H.L. Ni, T.J. Zhu, X.B. Zhao, Physica B 364 (2005) 50–54.
[21] Y.B. Xu, Z.M. Ren, W.L. Ren, K. Deng, Y.B. Zhong, Mater. Lett. 62 (2008) 763–766.
[22] G.Q. Zhang, W. Wang, X.L. Lu, X.G. Li, Cryst. Growth Des. 9 (2009) 145–150.
[23] X.B. Zhao, X.H. Ji, Y.H. Zhang, B.H. Lua, J. Alloys Compd. 368 (2004) 349–352.